

Influence of molecular hydrogen on Ge island nucleation on Si(001)

D. Dentel,^{a)} L. Vescan, O. Chrétien, and B. Holländer

Institut für Schicht- und Ionentechnik, Forschungszentrum Jülich GmbH, D-52425 Jülich, Germany

(Received 19 April 2000; accepted for publication 16 August 2000)

The influence of molecular hydrogen (H_2) on the structural and optical properties of self-assembled Ge dots grown on Si(001) has been studied using atomic force microscopy and photoluminescence spectroscopy (PL). Without hydrogen, a well known bimodal island size distribution occurs with small {105} faceted *pyramids*, and larger multifaceted *domes*. In the presence of an additional H_2 flow, we observe that a higher density of smaller pyramids and a lower density of domes occurs. Moreover, in the presence of hydrogen, PL investigations have revealed a thicker wetting layer thickness, probably due to a reduction of the surface diffusion length. © 2000 American Institute of Physics. [S0021-8979(00)07822-1]

I. INTRODUCTION

The strain-driven self-assembled formation of nanostructures has attracted a lot of interest in recent years because these new structures are expected to have better optical and electrical properties than those of conventional two-dimensional (2D) structures.¹ In order to obtain an improvement of these properties, it is necessary to fabricate these quasiozero-dimensional structures *in situ* without the need for a sophisticated structuring technology. One of the most prominent mechanisms is the Stranski–Krastanov growth mode in a lattice-mismatched heteroepitaxy, which leads to the formation of coherent three-dimensional (3D) islands after the growth of a 2D wetting layer. With a lattice mismatch of 4.2% between Si and Ge, it is the case for the growth of Ge on Si(001).^{2–4}

However, the islands can be used more effectively if they are uniformly sized. Of course, the kinetic growth conditions are critical. That is why a perfect knowledge of each growing parameter and its influence on energetic and thermodynamic surface properties, surface morphology, and island nucleation is an indispensable prerequisite. One of these parameters is the supply of an additional hydrogen flow. Several studies have investigated the influence of atomic hydrogen (H) on the heteroepitaxial growth of Ge/Si(001) and have demonstrated that the adsorbed H acts as a surfactant by increasing the thickness of the wetting layer^{5–8} (the growth mode transition from a 2D layer by layer to a 3D is delayed) and by reducing Ge surface segregation^{8–10} during the deposit of a Si cap layer. Only few studies were devoted to investigating the influence of molecular hydrogen (H_2), particularly the effect on Ge surface segregation.^{11–13}

As molecular hydrogen is very often used as carrier gas, particularly in various chemical vapor deposition (CVD) methods, it seems to be indispensable to take into account this parameter. In this article we want to show the influence of molecular hydrogen on the island nucleation and their size distribution. We have performed several experiments with and without an additional molecular hydrogen flow. Experi-

ment details are presented in Sec. II, and the atomic force microscopy (AFM) and photoluminescence spectroscopy (PL) results are presented and discussed in Sec. III and IV, respectively.

II. EXPERIMENT

The growth was carried out in a low pressure chemical vapor deposition (LPCVD) system, described elsewhere with more details,¹⁴ using dichlorosilane ($SiCl_2H_2$) as the Si source and He-diluted germane (GeH_4) as the Ge source (90% diluted). The total pressure in the reactor was varied in the range of 0.02–1 Torr as a function of the H_2 flow, used here as carrier gas. The GeH_4 flow, 1 sccm, was kept constant in all experiments corresponding to a growth rate of about $3.2 \pm 0.3 \text{ nm min}^{-1}$.

After the deposition of a 200 nm Si buffer layer at 800 °C, a Ge film of 6–8 equivalent ML (1 ML = 1.415 Å) was grown at 700 °C without H_2 and with an additional H_2 flow of 200 and 1000 sccm, respectively. At the end of the growth, the samples are immediately cooled with a cooling rate of 1° s^{-1} allowing a sufficient temperature quenching. This average thickness was chosen because it lies above the Stranski–Krastanov critical thickness (3–4 equivalent ML) and below the appearance of dislocations, the beginning of plastic relaxation. For PL experiments, the Ge deposited films were capped with a Si layer aimed to suppress nonradiative recombination at the Ge islanded surface. In order to preserve the buried islands, the Si cap layer was immediately deposited after the Ge layer (without a vent step of 1 min usually carried out in CVD) using the same growing conditions: temperature (700 °C) and H_2 flow (0, 200, and 1000 sccm, respectively). The islanded surface morphology was investigated with an AFM setup (Digital Instruments Nanoscope IIIa) operating in tapping mode. PL measurements were performed at low temperatures using a Fourier transform spectrometer (BIO-RAD FTS 40) equipped with an Ar^+ laser (power density of 5 W cm^{-2}). The average Ge layer thicknesses were determined by Rutherford backscattering spectroscopy (RBS).

^{a)}Electronic mail: d.dentel@fz-juelich.de

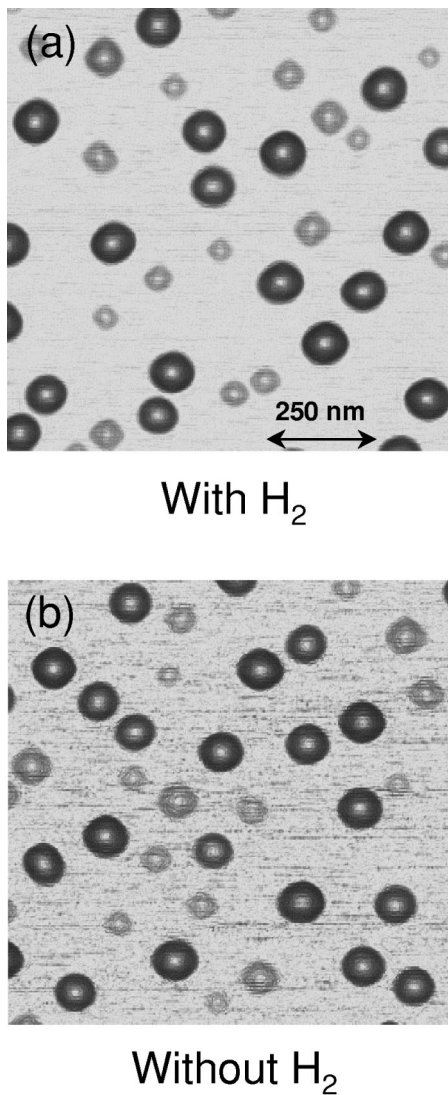


FIG. 1. $1\ \mu\text{m} \times 1\ \mu\text{m}$ atomic-force micrographs of (a) a 6.6 eq ML Ge film grown at $700\ ^\circ\text{C}$ with an additional H_2 flow of 1000 sccm (sample No. 1615), and (b) a 6.8 eq-ML Ge film grown at $700\ ^\circ\text{C}$ without H_2 (sample No. 1620).

III. ATOMIC FORCE MICROSCOPY

Figures 1(a) and 1(b) display AFM pictures of the islanded surface morphology obtained with and without a 1000 sccm H_2 flow, respectively. With 6.6–6.8 equivalent ML of Ge, as already pointed out by several authors,^{4,15–17} a bimodal size and shape distribution of Ge islands is obtained. Small square based islands, so-called *pyramids*, having {105} facets coexist with larger rounded multifaceted *domes*. At first sight, there is no great difference between the two final

morphologies. The density of pyramids (ρ_{pyramids}) and that of domes (ρ_{domes}) are approximately unchanged with an additional molecular hydrogen flow (Table I).

The main difference lies in the dimension of the island. The corresponding island height and diameter are shown in Fig. 2. The bimodality is also clearly evidenced. For a better representation of the growing condition influence on the mean height and the mean base dimensions of pyramids and domes, we have fitted the obtained histograms with two gaussian curves, corresponding to each kind of island. In the presence of H_2 , the pyramid dimensions are reduced. With H_2 , the mean height of the pyramids, is about $4.0\ \text{nm} \pm 0.7\ \text{nm}$ [Fig. 2(a)] while the one without H_2 , is higher: $5.8 \pm 0.7\ \text{nm}$ [Fig. 2(c)]. This is also true for the pyramid base dimensions (with H_2 , $b^{av} = 63 \pm 4\ \text{nm}$ and without H_2 , $b^{av} = 72 \pm 4\ \text{nm}$ [Figs. 2(b) and 2(d)]. The estimated error is due to the spatial resolution of the AFM software. This detailed statistical analysis, performed on large surface areas ($20\ \mu\text{m}^2$), is summarized in Table I. These AFM measurements show that the dome nucleation process seems to be less influenced than that of the pyramid with an additional H_2 flow. But we can still observe a reduction of the island dimensions (Fig. 2 and Table I).

With our high-vacuum LPCVD system, different species are present in the reactor: germane (GeH_4) used as Ge source, helium (He) in which GeH_4 is diluted (90% He and 10% GeH_4) and H_2 used as carrier gas. Before discussing the effect of molecular hydrogen, we have to reply to the following question: why can the reduction of the island dimensions not be due to atomic hydrogen? We present three reasons on that query.

(1) Atomic hydrogen only comes from the dissociation of germane on the surface. As molecular hydrogen is supposed to be very stable, its dissociation can only be obtained at very high temperature (above $1500\ ^\circ\text{C}$).

(2) If atomic hydrogen should explain our observations, its influence (reduction of surface diffusion and surface segregation) would be obviously increased, and a more planar growth would be promoted, with a higher partial pressure of atomic hydrogen (P_{H}). With our growing conditions, this is not the case, but the opposite is valid because P_{H} is higher without H_2 than with H_2 . In fact, as a complete dissociation of germane occurs, without the formation of germane-related radicals,¹⁸ P_{H} is given by

$$P_{\text{H}} = 4(P_{\text{GeH}_4}) = 4(P_{\text{tot}}) \frac{\phi_{\text{GeH}_4}}{\phi_{\text{GeH}_4} + \phi_{\text{H}_2} + \phi_{\text{He}}}, \quad (1)$$

where P_{tot} is the total pressure and ϕ_X the flow of each gas present in the reactor (the values of all these parameters are

TABLE I. Summary of RBS and AFM analysis on the uncapped samples.

Sample No.	H_2 flux (sccm)	RBS thickness (equivalent ML)	ρ_{pyramids} ($10^8\ \text{cm}^{-2}$)	ρ_{domes} ($10^8\ \text{cm}^{-2}$)	$h_{\text{pyramids}}^{\text{av}}$ (nm)	$h_{\text{domes}}^{\text{av}}$ (nm)	$b_{\text{pyramids}}^{\text{av}}$ (nm)	$b_{\text{domes}}^{\text{av}}$ (nm)
1615	1000	6.6 ± 0.5	20	16	4.0	16.2	63	101
1620	0	6.8 ± 0.5	17	19	5.8	17.1	72	104

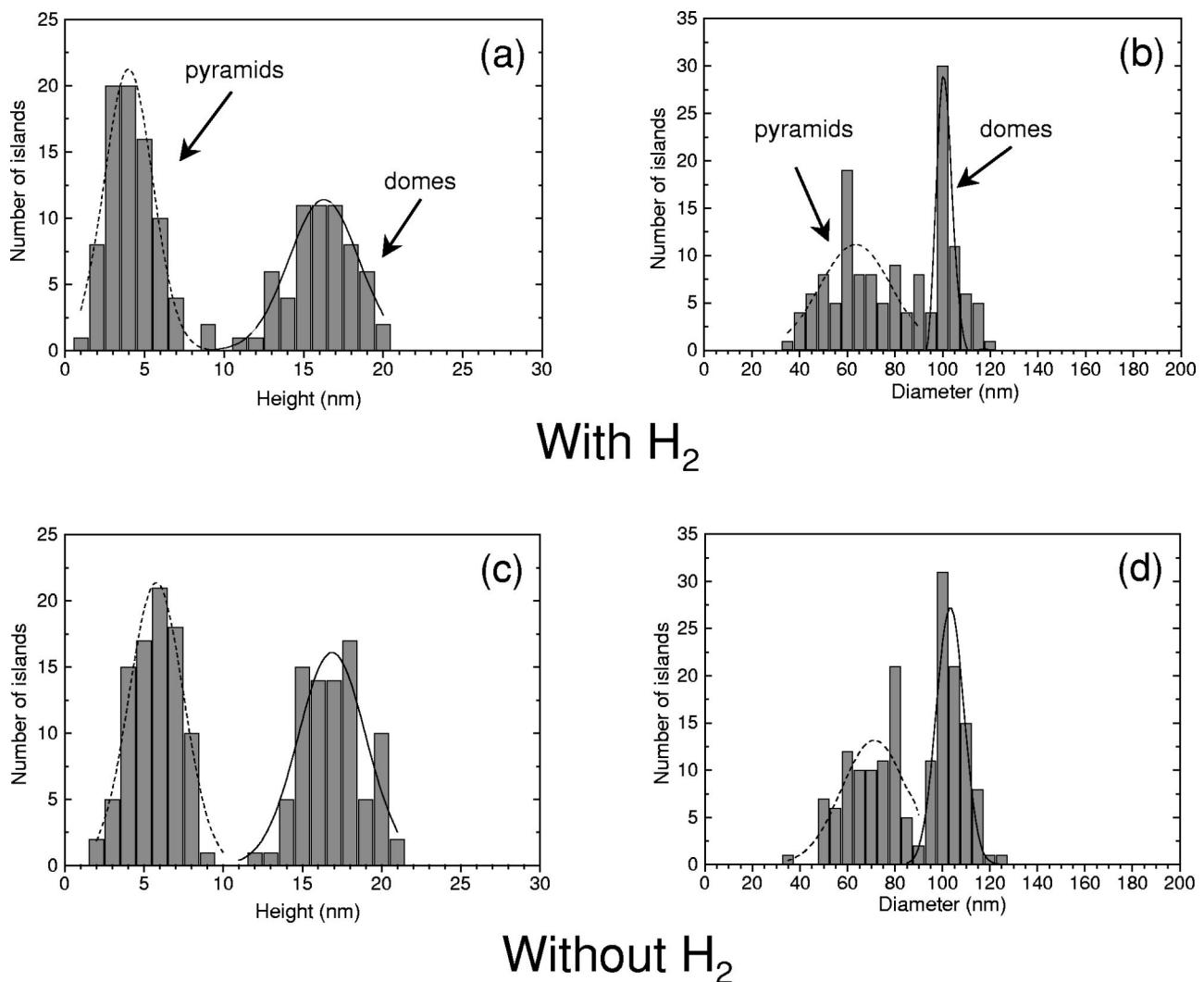


FIG. 2. Distribution of island heights (a) [(c)] and base dimensions (b) [(d)] of the sample No. 1615 grown with H_2 [sample No. 1620 grown without H_2]. Statistical analysis was performed on a large surface area ($20 \mu m^2$).

given in the previous section). Without H_2 , P_H is about 8×10^{-3} Torr, when with H_2 , P_H is about 4×10^{-3} Torr.

(3) The deposition temperature ($700^\circ C$) is much higher than the desorption temperature of hydrogen from a Ge surface ($\approx 300^\circ C$) or a Si one ($\approx 500^\circ C$).¹⁹ The residence time of atomic hydrogen on the growing surface is accordingly probably too low and cannot explain these differences.

We are forced to conclude that molecular hydrogen has an effect on island nucleation and consequently on surface diffusion. In previous works, Eaglesham *et al.*⁹ and Copel and Tromp¹⁰ have demonstrated that molecular hydrogen acts in reducing Ge surface segregation. It was described in a two-state exchange model²⁰ by an increasing of the segregation energetic barrier. Additionally, we demonstrate here that molecular hydrogen, as well as atomic H, has a kinetic effect in the dynamical process of island nucleation: *the reduction of the surface diffusion length*. However, in order to explain the influence of H_2 on pyramid nucleation and the weaker influence on dome nucleation, we have to consider that the equilibrium shape of pyramids and domes are differently influenced by kinetics. Goryll *et al.*¹⁷ have also pointed out the strong dependence of pyramid density and the weaker depen-

dence of the domes density on the deposition rate, another important kinetic growth parameter.

Moreover, equilibrium calculations about the interaction between molecular hydrogen and a silicon surface predict a strong increase of the fraction of surfaces sites occupied by hydrogen by increasing the total pressure.²¹ For instance, at $700^\circ C$, the hydrogen coverage should be about 20% for 1×10^{-3} Torr and about 96% for 10 Torr. With these predictions, in our range of pressures (0.02–1 Torr), the hydrogen coverage should vary between 50% and 93%. In spite of the relatively high deposition temperature, we have to take into account the assumption of a surface reaction between molecular hydrogen and the silicon surface [$H_2(g) + Si(\text{empty site}) \rightleftharpoons 2HSi(ads)$] to try to explain the observed lack of adatoms diffusivity on the growing surface.

IV. PHOTOLUMINESCENCE SPECTROSCOPY

In order to study the influence of hydrogen on the optical properties, we have performed PL investigations on the corresponding Si-capped samples. Figure 3 displays the 5 K PL spectra of three Ge layers grown, respectively, with an addi-

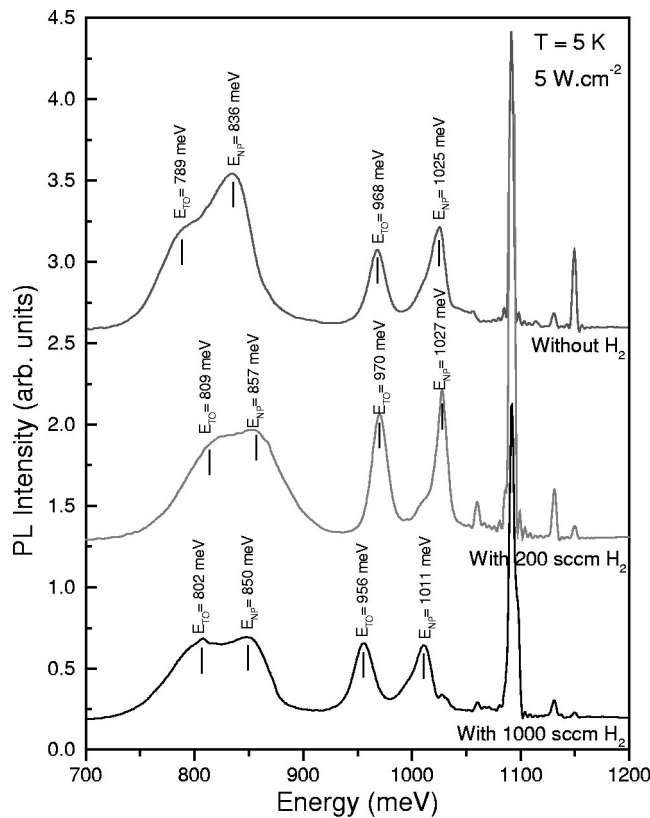


FIG. 3. 5 K photoluminescence spectra of a buried Ge film grown, respectively, with 200 sccm, 1000 sccm H_2 , and without H_2 . Wetting layer and island-related peaks corresponding to the NP and TO transition energies are identified on each spectrum.

tional H_2 flow of 1000, 200, and 0 sccm. Two pairs of PL peaks are clearly visible, each consisting of a nonphonon (NP) transition and a transverse optical phonon (TO) replica. The pair at the lower energy side of the spectra stems from the self-assembled islands, and on the high energy side, the peaks are attributed to the 2D wetting layer.^{22,23}

Table II summarizes the RBS and PL analysis of the three investigated samples. As the Ge layer grown with 200 sccm H_2 is thinner in comparison with the other ones, the PL spectra labeled “with 200 sccm H_2 ” in Fig. 3 will not be taken into account for the discussion about the influence of H_2 on the PL signature. We will consider this sample only in the last part of our discussion about the temperature dependence of the PL intensity.

For samples 1616 (with 1000 sccm H_2) and 1621 (without H_2), a different behavior of each pair of peaks can be noticed. A blue shift (red shift) occurs in the presence of molecular hydrogen for the PL signal who stems from the self-assembled islands (the wetting layer). The NP energy

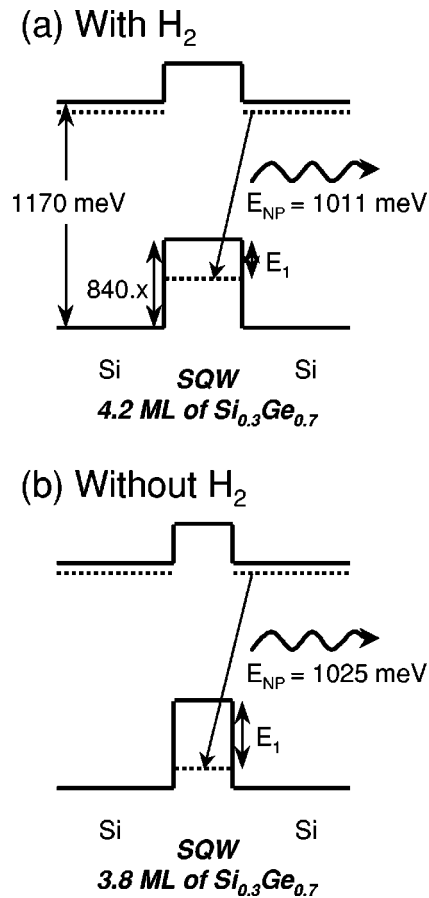


FIG. 4. Schematic representation of radiative recombination process in thick (a) and thinner (b) Ge SQW. These two situations exhibit the supposed mechanisms occurring in the 2D wetting layer of samples No. 1616 (with H_2) and No. 1621 (without H_2).

transition related to the wetting layer shifts from 1011 meV (with H_2) until 1025 meV (without H_2), when at the same time the one related to islands decreases from 850 meV (with H_2) until 836 meV (without H_2). The blue shift, concerning the 2D layer-related signal, can be explained by different wetting layer thicknesses. Indeed, for a single quantum well (SQW), the NP peak position is defined as (Fig. 4):

$$E_{NP} = E_G^{Si} - E_{ex} - \Delta E_V + E_1, \quad (2)$$

where E_G^{Si} is the silicon gap (=1170 meV); E_{ex} is the exciton binding energy in Si (=14 meV); ΔE_V is the valence band offset for strained $Si_{1-x}Ge_x$ Si layers (=840x, x is the Ge concentration)²⁴ and E_1 is the hole confinement energy. As E_1 strongly depends on the SQW thickness we are able to estimate the 2D wetting layer thickness by evaluating this confinement energy. The following assumptions were made:

TABLE II. Summary of RBS and PL analysis on the 80 nm Si-capped samples.

Sample No.	H_2 flux (sccm)	RBS thickness (equivalent ML)	E_{NP}^{2D} (meV)	E_{TO}^{2D} (meV)	E_{NP}^{3D} (meV)	E_{TO}^{3D} (meV)	Estimated wetting layer thickness (ML)
1616	1000	8.0 ± 0.5	1011	956	850	802	4.2 ± 0.1
1617	200	5.7 ± 0.5	1027	970	855	809	3.7 ± 0.1
1621	0	7.9 ± 0.5	1025	968	836	789	3.8 ± 0.1

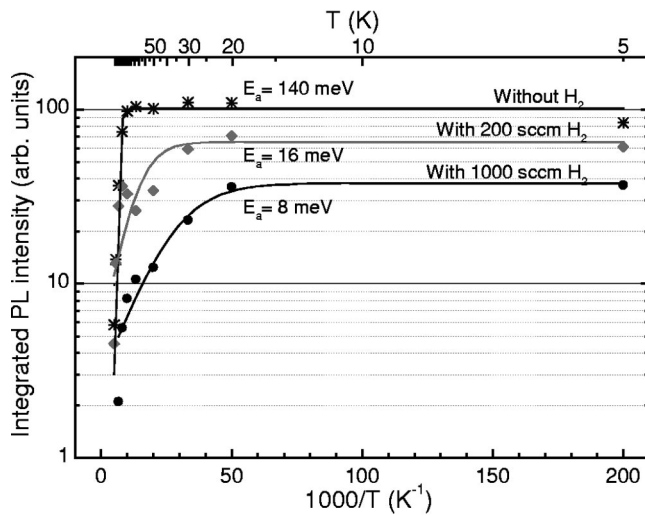


FIG. 5. Temperature dependence of the integrated PL intensity related to the islands for the three investigated samples: No. 1616 (with 1000 sccm H₂), No. 1617 (with 200 sccm H₂), and No. 1621 (without H₂).

(a) the SQW is strained, and (b) the effective mass of holes for strained Si_{1-x}Ge_x, along the [001] direction, was calculated with the formula²⁵

$$m_{hh} = 0.2907 - 0.09021 \cdot x + 0.00552 \cdot x^2. \quad (3)$$

By assuming a low intermixing (approximately 30% as considered elsewhere)²⁶ we have estimated the wetting layer thickness at 4.15 and 3.80 eq ML (1 ML = 1.398 Å) with and without H₂ respectively (Table II). These values are not absolute values. Nevertheless, the growing film seems to have a thicker wetting layer in the presence of molecular hydrogen. This is a direct consequence, and then also a confirmation, of the assumption made in the previous section about the reduction of the surface diffusion in presence of a dynamic H₂ flow. If we consider the signal related to the self-assembled islands, the observed shift to lower energies without H₂ can be attributed to the nucleation of bigger coherent islands, elastically more relaxed, and probably due to a higher surface diffusion and an earlier growth mode transition.

Moreover, with an increased molecular hydrogen flow, the dots PL intensity is lower. Under such growth conditions, with a lack of diffusivity for adatoms, more defects (stacking faults, vacancies, etc.) are probably present at the growing surface and into the islands.

Figure 5 displays the temperature dependence, in a range between 5 and 200 K, of the islands related PL intensity for the three investigated Si-capped samples. Two observations can be made here. At first, as already pointed out in Fig. 3, the islands PL intensity dependence on an additional H₂ flow is confirmed here for each temperature. Moreover, by comparing the results obtained with and without H₂, a differentiated behavior of the PL intensity as a function of the temperature is clearly evidenced. Without H₂, the intensity drops rapidly above 100 K, when with a H₂ flow (200 and 1000 sccm), it decreases slowly beyond 20 K.

We have tried to estimate the activation energy of the nonradiative recombination process with a simplified phe-

nomenological model of Sturm *et al.*²⁷ In this model, the integrated PL intensity is given by

$$I_{\text{Ge}} \propto \frac{1}{1 + \gamma \cdot e^{-E_a/kT}}, \quad (4)$$

where

$$\gamma = \frac{\tau_{\text{Ge}} \cdot W_{\text{Si}}}{\tau_{\text{Si}} \cdot W_{\text{Ge}}}. \quad (5)$$

τ_{Ge} (τ_{Si}) is the nonradiative lifetime in Ge (in Si). W_{Ge} is the width of the Ge layer (1.1 nm) and W_{Si} is the effective width of the Si in which the photogenerated carriers reside (by taking into account our excitation power, $W_{\text{Si}} \approx 3-5 \mu\text{m}$).

We can observe a strong decrease of the activation energy with the supply of a molecular hydrogen flow. In order to explain such a difference between island nucleation with and without H₂, we have to give some additional explanations. In the used model, the varying parameters (fitting parameters) are E_a and the ratio $\tau_{\text{Ge}}/\tau_{\text{Si}}$. Without H₂, the value of 140 meV for the activation energy was obtained by considering $\tau_{\text{Ge}}/\tau_{\text{Si}} \approx 1$. On the other hand, with H₂, a good fit of the experimental data was only possible with $\tau_{\text{Ge}}/\tau_{\text{Si}} \approx 10^{-4}$ (it means $\tau_{\text{Ge}} \ll \tau_{\text{Si}}$). For silicon and germanium the carrier nonradiative lifetimes are given by

$$\tau \propto \frac{1}{N \cdot \sigma}, \quad (6)$$

where N is the concentration of the nonradiative recombination center (impurities or defects) and σ is the electron or hole capture cross section in Si or Ge. As the capture cross section values of impurities and defects in Si and Ge are quite similar,²⁸ the difference of 4 order of magnitude for the ratio $\tau_{\text{Ge}}/\tau_{\text{Si}}$ with and without H₂ can probably be explained by assuming a higher concentration of defects in the Ge layer who was grown with the supply of a H₂ flow.

Then, as previously mentioned and confirmed here, by increasing the H₂ flow, the reduction of surface diffusion prevails the occurrence of a high concentration of defects (stacking faults, vacancies, etc.) which act as carrier traps and nonradiative recombination centers.

V. CONCLUSION

This article summarizes our investigations about the influence of an additional molecular hydrogen flow on morphologies and optical properties of strained Ge layers. Our AFM investigations have revealed that with H₂, the bimodality is preserved and nucleation of smaller islands occur. Similar to atomic hydrogen, H₂ acts in reducing the surface diffusion length. The PL analysis seems to confirm this point. Indeed, the observed red shift of wetting layer-related pair of peaks (blue shift of islands-related pair of peaks) can be attributed to a thicker 2D layer (nucleation of smaller islands). An additional consequence of the reduced surface diffusion in the presence of molecular hydrogen, clearly pointed out by the temperature dependence of the PL intensity, is the occurrence of more nonradiative recombination

center (defects). Moreover, the nucleation process of pyramids is probably more influenced by kinetic growing parameters than the one of domes.

ACKNOWLEDGMENTS

The authors thank M. Goryll and K. Grimm for kind help in AFM and PL investigations and T. Stoica for helpful discussions. The financial support from the TMR Network Aapples No. FMRXCT96-0029 is gratefully acknowledged by two of the authors (D.D. and O.C.).

- ¹For a review, see, e.g., G. Abstreiter, P. Schittenhelm, C. Engel, E. Silveira, A. Zrenner, D. Meertens, and W. Jäger, *Semicond. Sci. Technol.* **11**, 1521 (1996), and references therein.
- ²D. J. Eaglesham and M. Cerullo, *Phys. Rev. Lett.* **64**, 1943 (1990).
- ³Y.-W. Mo, D. E. Savage, B. S. Swartzentruber, and M. G. Lagally, *Phys. Rev. Lett.* **65**, 1020 (1990).
- ⁴G. Medeiros-Ribeiro, A. M. Bratkovski, T. I. Kamins, D. A. A. Ohlberg, and R. S. Williams, *Science* **279**, 353 (1998).
- ⁵A. Sakai and T. Tatsumi, *Appl. Phys. Lett.* **64**, 52 (1994).
- ⁶S.-J. Kahng, J. Y. Park, K. H. Booh, J. Lee, Y. Khang, and Y. Kuk, *J. Vac. Sci. Technol. A* **15**, 927 (1997).
- ⁷D. Dentel, J. L. Bischoff, T. Angot, and L. Kubler, *Surf. Sci.* **402–404**, 211 (1998).
- ⁸K. Oura, V. G. Lifshits, A. A. Saranin, A. V. Zotov, and M. Katayama, *Surf. Sci. Rep.* **35**, 1 (1999), and references therein.
- ⁹D. J. Eaglesham, F. C. Unterwald, and D. C. Jacobson, *Phys. Rev. Lett.* **70**, 966 (1993).
- ¹⁰M. Copel and R. M. Tromp, *Appl. Phys. Lett.* **58**, 2648 (1991).
- ¹¹K. Nakagawa, A. Nishida, Y. Kimura, and T. Shimada, *Jpn. J. Appl. Phys., Part 2* **33**, L1331 (1994).
- ¹²Z. Rong, H. Hongbin, G. Shulin, Y. Kai, S. Yi, W. Ronghua, Z. Youdou, and F. Duan, *Mater. Res. Soc. Symp. Proc.* **342**, 63 (1994).
- ¹³G. Onta, S. Fukatsu, Y. Ebuchi, T. Hattori, N. Usami, and Y. Shiraki, *Appl. Phys. Lett.* **65**, 2975 (1994).
- ¹⁴L. Vescan, W. Jäger, C. Dieker, K. Schmidt, and H. Lüth, *Mater. Res. Soc. Symp. Proc.* **263**, 23 (1992).
- ¹⁵M. Tomitori, K. Watanabe, M. Kobayashi, and O. Nishikawa, *Appl. Surf. Sci.* **76/77**, 322 (1994).
- ¹⁶T. I. Kamins, E. C. Carr, R. S. Williams, and S. J. Rosner, *J. Appl. Phys.* **81**, 211 (1997).
- ¹⁷M. Goryll, L. Vescan, and H. Lüth, *Mater. Res. Soc. Symp. Proc.* **570**, 205 (1999).
- ¹⁸B. Cunningham, J. O. Chu, and S. Akbar, *Appl. Phys. Lett.* **59**, 3574 (1993).
- ¹⁹For a review, see, T. Angot and P. Louis, *Phys. Rev. B* **60**, 5938 (1999), and references therein.
- ²⁰J. J. Harris, D. E. Ashenford, C. T. Foxon, P. J. Dobson, and B. A. Joyce, *Appl. Phys. A: Mater. Sci. Process.* **33**, 87 (1984).
- ²¹D. A. Grützmacher, T. O. Sedgwick, L. Scandella, A. Zaslavsky, A. R. Powell, and S. S. Iyer, *Vacuum* **46**, 947 (1995).
- ²²H. Sunamura, N. Usami, Y. Shiraki, and S. Fukatsu, *Appl. Phys. Lett.* **66**, 3024 (1995).
- ²³P. Schittenhelm, M. Gail, J. Brunner, J. F. Nützel, and G. Abstreiter, *Appl. Phys. Lett.* **67**, 1292 (1995).
- ²⁴C. G. Van de Walle and R. Martin, *Phys. Rev. B* **34**, 5621 (1986).
- ²⁵R. Loo *et al.*, *Phys. Rev. B* **50**, 18113 (1994).
- ²⁶L. Vescan, M. Goryll, T. Stoica, K. Grimm, O. Chrétien, E. Mateeva, C. Dieker, and B. Holländer, *Appl. Phys. A* (to be published).
- ²⁷J. C. Sturm, A. St. Amour, Q. Mi, L. C. Lenchyshyn, and M. L. W. Thewalt, *Jpn. J. Appl. Phys., Part 1* **33**, 2329 (1994).
- ²⁸A. Dargys and J. Kundrotas, *Handbook on Physical Properties of Ge, Si, GaAs, and InP* (Science and Encyclopedia Publishers, Vilnius 1994).